JREE: Vol. 12, No. 4, (Autumn 2025) 64-73

Journal of Renewable Energy and Environment

Journal Homepage: www.jree.ir

Materials and Energy Research Center

MERC

Research Article

Wind Energy Conversion System Coupled with High Gain Boost Converter Using Grey Wolf Optimization Based Maximum Power Point Tracking Approach for High Voltage Direct Current Transmission System

Sudha B, S. Nagaraja Rao*

Department of of Electrical Engineering, Faculty of Engineering & Technology, M S Ramaiah University of Applied Sciences, Bangalore, India.

PAPER INFO

Paper history:
Received: 07 April 2025
Revised: 25 June 2025
Accepted: 22 September 2025

Keywords:
GWO,
MPPT,
TLBC,
Voltage Gain

ABSTRACT

In this paper, a Wind Energy Conversion System (WECS) coupled with a Three-Level Boost Converter (TLBC) using a Grey Wolf Optimization (GWO)-based Maximum Power Point Tracking (MPPT) approach is studied. The proposed WECS is designed for HVDC transmission line applications and is connected to the grid. It consists of two power converters: a TLBC and an unregulated rectifier. The TLBC is employed to increase the voltage gain, while an unregulated rectifier, powered by a Permanent Magnet Synchronous Generator (PMSG), is used for AC-to-DC conversion. Furthermore, a metaheuristic optimization method, namely the GWO-based MPPT approach, is applied to determine the optimal power point for the TLBC powered by the PMSG-based WECS. The system's performance is evaluated under both fixed and variable wind speed profiles, specifically at 8 m/s, 10 m/s, and 12 m/s. The wind-powered TLBC with the GWO-based MPPT approach is modeled, simulated, and tested in MATLAB®/Simulink®. In addition, the proposed wind-powered TLBC with the GWO-based MPPT approach is compared with the traditional Perturb & Observe (P&O) method. The performance of the TLBC is assessed in terms of voltage gain, output ripple, settling time, and accuracy of the PMSG-based WECS. The proposed system demonstrates superior performance, achieving a high voltage gain with a boost factor of 5.996, minimal oscillations, improved settling time, and high accuracy of 99%, compared with the P&O-based MPPT approach.

https://doi.org/10.30501/jree.2025.512594.2304

1. INTRODUCTION

Wind power occupies a foremost position in research on new energy generation, and its production share is rising steadily. Wind energy remains a clean and widely utilized resource. In India, it serves as a primary source for peak power generation and helps reduce dependence on fossil fuels, thereby contributing to a more sustainable environment (Catalán P. et al., 2023). The rapid development of Electric Vehicles (EVs) has further increased attention toward renewable energy resources for EV applications within the research domain.

The fundamental principle of wind power generation lies in harnessing wind energy and converting it into mechanical energy through turbines, which is subsequently transformed into electrical energy via wind turbine generators. Together, these components form the Wind Energy Conversion System (WECS) (Kiran K. B. et al., 2021).. The output of WECS can be directly supplied to the power grid, High Voltage Direct Current (HVDC) transmission lines, and end-users. HVDC transmission requires very high voltage for efficient long-distance power transfer. Compared to High Voltage Alternating Current (HVAC), HVDC offers several advantages, including fewer conductors, smaller tower size, reduced corona effect, lower losses, and higher reliability.

Currently, the most widely used wind generators in WECS are Doubly Fed Induction Generators (DFIGs) and Permanent Magnet Synchronous Generators (PMSGs). A key control challenge in WECS is Maximum Power Point Tracking (MPPT). Much research has focused on metaheuristic-based MPPT approaches for WECS and DC–DC boost converters. MPPT methods are applied below rated wind speeds (Pande J. et al., 2021) and include techniques such as power signal feedback, optimal Tip Speed Ratio (TSR), and Hill Climbing Search (HCS) (Mousa H.H. et al., 2021).

Global energy challenges, such as environmental pollution and energy crises, have intensified the demand for renewable energy sources. Renewable energy—derived from solar, wind, hydro, and biomass systems—depends on resource availability and can be categorized into mechanical, electromagnetic, and thermal forms. Wind energy can be converted into mechanical energy for applications such as water pumping, or into electrical energy using alternators. The growing demand for industrial energy has made Renewable Energy Systems (RES) increasingly important worldwide

*Corresponding Author's Email: nagarajarao.ee.et@msruas.ac.in (S. Nagaraja Rao)
URL: https://www.jree.ir/article_230121.html

Please cite this article as: S, B. & Rao, S. N. (2025). Wind Energy Conversion System Coupled with High Gain Boost Converter Using Grey Wolf Optimization Based Maximum Power Point Tracking Approach for High Voltage Direct Current Transmission System. *Journal of Renewable Energy and Environment (JREE)*, 12(4), 64-73. https://doi.org/10.30501/jree.2025.512594.2304

(Haque et al, 2008). Wind energy, in particular, is considered one of the most reliable RES options for both environmental and commercial applications. Its environmentally friendly nature has positioned WECS as a leading RES (Pranupa S. et al., 2024).

However, wind energy output varies due to continuously changing wind speeds (Hajer Gaied et al., 2022). The power output of WECS depends directly on wind speed availability. Therefore, effective MPPT methods are essential for extracting maximum power from PMSG-based WECS (Veerabhadra, J., & Rao, S. N., 2023). Maintaining continuous WECS operation connected to the grid or load is challenging due to fluctuations in turbine capacity utilization (Rajapandian, B., & Sundarrajan, 2020). The MPPT approach is critical to ensure consistent operation, though metaheuristic MPPT techniques have both advantages and limitations (Sarang et. al., 2024).

Variable-speed and constant-frequency technologies are commonly applied in WECS. The MPPT approach is particularly important for variable-speed, fixed-frequency systems (Priyadarshi N. et al., 2019). WECS has also proven valuable in remote areas because of its economic and environmental advantages compared to other RES options. Many studies have examined small-scale WECS using PMSGs and DFIGs (Pranupa S. et al., 2023). PMSGs, in particular, are highly reliable, require minimal maintenance, do not need gearboxes, and exhibit higher efficiency (Das M. and Agarwal V., 2016). To consistently extract maximum power under varying environmental conditions, metaheuristic MPPT approaches are employed.

MPPT strategies can generally be categorized into direct and indirect approaches (Pranupa S. et al., 2022 and Teklehaimanot et. al., 2024). Direct approaches, such as HCS and Fuzzy Logic Controllers (FLC), operate autonomously based on generator characteristics and meteorological conditions (Ahmad R. and Abdul-Hussain M., 2017). Indirect approaches rely on generator features such as Optimal Torque Control (OTC) and Power Factor Stability (PSF) (Nagaraja Rao S. et al., 2022).

This paper focuses on a novel TLBC design to enhance voltage gain, combined with a metaheuristic GWO-based MPPT approach to identify the optimal operating point for a PMSG-based WECS connected to an HVDC transmission line. The TLBC achieves up to a sixfold increase in voltage gain and exhibits significantly reduced ripple content compared to conventional DC–DC converters. The proposed PMSG-based WECS coupled with a TLBC using the GWO-based MPPT approach is simulated in MATLAB®/Simulink®. The system is evaluated under both fixed wind speed (10 m/s) and variable wind speed profiles (8 m/s, 10 m/s, and 12 m/s).

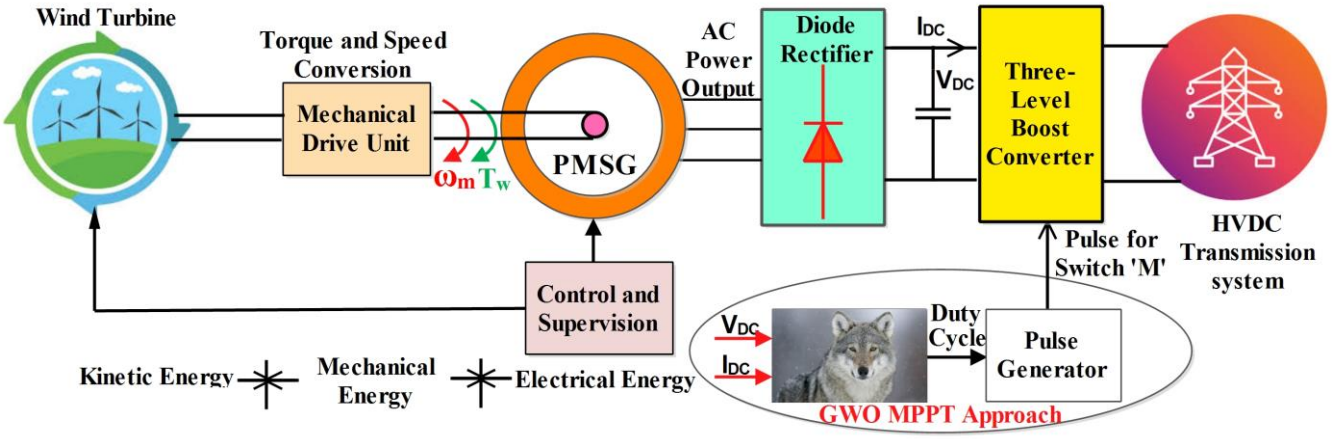

Figure 1. Proposed WECS interfaced with TLBC for HVDC transmission line.

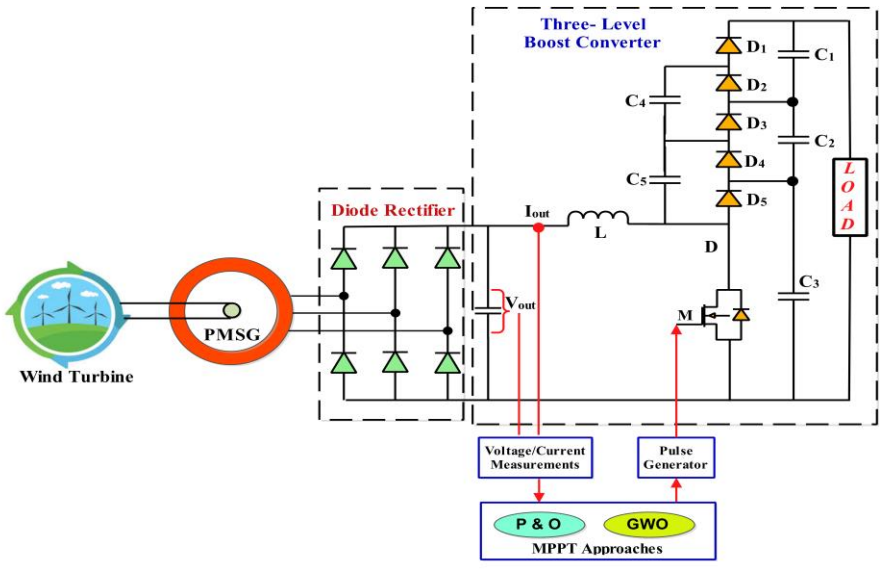

Figure 2. TLBC with PMSG based WECS using GWO MPPT approach.

2. PROPOSED SYSTEM CONFIGURATION

The block diagram representation of the proposed WECS is shown in Figure 1. The performance of the WECS interfaced with the TLBC, employing the metaheuristic GWO-based MPPT approach for HVDC transmission line applications, is demonstrated. The wind turbine is designed according to selected specifications, and its characteristics are analyzed using MATLAB®/Simulink®. The mechanical output of the wind turbine is supplied to the PMSG, whose AC output power is converted to DC using a diode rectifier. The rectified PMSG output is then boosted using the TLBC. To achieve maximum power extraction, the metaheuristic GWO-based MPPT approach is employed. Finally, the maximized output is delivered to the HVDC transmission line. The circuit representation of the wind-powered TLBC with the metaheuristic GWO-based MPPT approach, coupled with the PMSG-fed rectifier-based WECS, is presented in Figure 2. The TLBC consists of an inductor, an Insulated Gate Bipolar Transistor (IGBT), a diode, and a capacitor for energy storage.

2.1 PMSG Based WECS

The variable-speed PMSG is coupled to an identical wind turbine (Ahmad R. and Abdul-Hussain M., 2017). The mechanical output of the turbine is analyzed, and both turbine torque and rotational speed are recorded. Figure 3 illustrates the mathematical model of the wind turbine, while Figure 4 shows the relationship between the power coefficient of the wind turbine (Cp) and the tip speed ratio (TSR, λ) for various pitch angles (β). The Cp value is 0.4105 when the pitch angle is zero. Eq.s (1) to (3) present the turbine modeling equations. The variation of the wind power coefficient Cp is evaluated for pitch angles of 0°, 2°, 4°, 6°, 8°, 10°, and 12°. For this study, pitch angles are considered within the range of 0° to 12°.

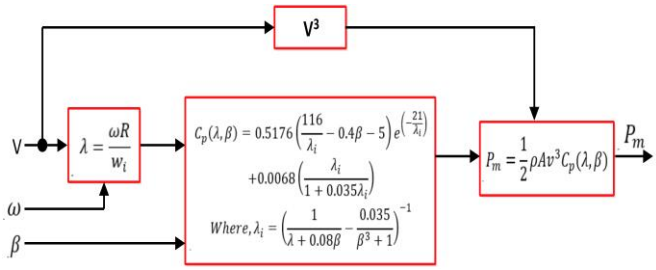

Figure 3. Wind turbine mathematical model.

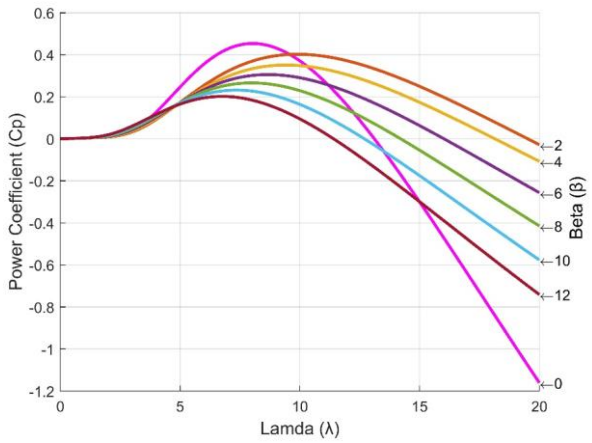

Figure 4. Wind Characteristics of Cp Vs λ (Lamda) for different pitch angles β (Beta).

Eq. (1) represents the power output of the wind turbine, where P_m is the mechanical output power, C_p is the wind turbine power coefficient, A is the swept area (m^2), Vm is the wind speed (m/s), ρ is the air density in $K_g m^2$, and ω_m is the rotor speed in rad/sec (Pranupa S et al., 2022 and Rao et. al., 2018).

$$P_m = \frac{1}{2} C_p(\lambda,\beta)\rho A V_w^3 \quad (1)$$

$C_p(\lambda,\beta)$, Wind turbine's Power Coefficient is given by Eq. (2).

$$C_p(\lambda,\beta) = C_1\left(\frac{C_2}{\lambda_I} - C_3\beta - C_4\beta^x - C_5\right)e^{-\frac{C_6}{\lambda_i}} \quad (2)$$

The rotor aerodynamic torque is given by Eq. (3):

$$T_\omega = \frac{P_m}{\omega_m} = \frac{\frac{1}{2}\rho A v^3 C_p(\lambda,\beta)}{\omega_m} = \frac{\frac{1}{2}\rho \pi R^2 v^3 C_p(\lambda,\beta)}{\omega_m} \text{ N-m} \quad (3)$$

Figure 5 presents the power characteristics of the turbine, illustrating how turbine power varies with angular velocity under different wind speeds, as well as the per-unit power characteristics.

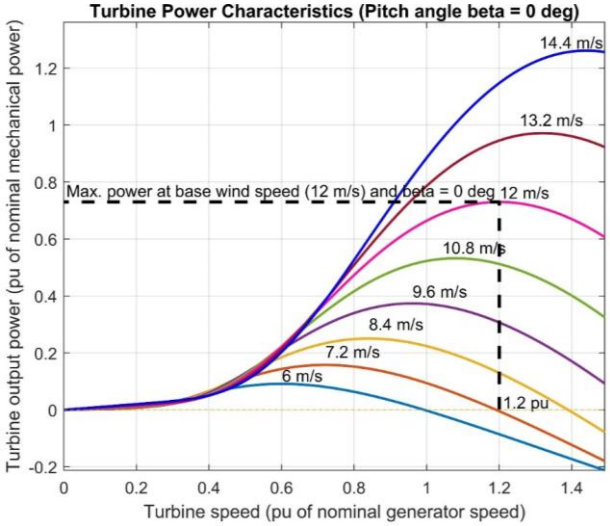

Figure 5. Turbine power characteristics at Pitch angle β=0°.

C_1 to C_6 are constants shown in Figure 3.

Radius, R=1.91431, Air density in $K_g m^2$, ρ=1.225, Sweft area in m^2, $A=\pi R^2$=11.506, Wind speed in m/s, V_w= 12 m/sec, for β=0, λ=8.1, λ_i= 11.304

Figure 2 illustrates the model of an uncontrolled diode rectifier integrated with a PMSG. The output of the PMSG-based WECS is transmitted to the load through the rectifier and TLBC (Nagaraja Rao et al., 2022). Eq. (4) consists of two components: the primary term represents the DC output voltage of the rectifier in the absence of commutation, while the secondary term accounts for the voltage drop caused by the commutation process involving synchronous reactance.

2.2 Three Level Boost Converter (TLBC)

A booster is necessary to raise the output voltage level, as very high DC voltage is required for HVDC transmission line applications. The conventional boost converter is insufficient for achieving such high voltage levels (Sulake et al., 2018). In this paper, a new TLBC converter is introduced. In this converter, the DC output voltage is boosted to three times the input voltage. The TLBC is suitable for both HVDC and AC grid applications. Standard DC–DC converters have restricted voltage output. Traditional DC–DC converters employ

expensive high-frequency transformers because of their limited power capabilities, and designing high-frequency transformers for high-power applications is exceedingly challenging (Mohamed S. A. and Abd El Sattar M., 2019). Conventional DC–DC converters can be configured in several ways to provide high voltage gain; however, they require significant maintenance.

Figure 6 illustrates the circuit configuration of a TLBC. The model enhances output voltage in three levels: Vdc × 2, Vdc × 4, and Vdc × 6, representing the three-level operation of the converter. It primarily consists of a conventional boost converter, five DC bus capacitors, and five diodes. The main advantage of the TLBC is its scalability: additional diodes and capacitors can be incorporated to extend the number of levels without altering the core circuit configuration. The voltage can be doubled without the use of transformers and with a relatively low duty ratio (D) (Rao et. al., 2018). The TLBC circuit operates in three stages. The absence of inductor power loss in the TLBC provides critical design benefits. The boost factor for a traditional voltage-gain boost converter is given in Eq. (5) (Pranupa S. et al., 2022).

$$\text{Voltage gain, } \frac{V_0}{V_{dc}} = \frac{1}{1-D} \tag{5}$$

V_0=output voltage, Vdc=input DC voltage, D=duty ratio. Since no loss system, voltage gain for N-level boost converter is calculated as follows:

$$\frac{V_0}{V_{dc}} = \frac{N}{1-D} \tag{6}$$

Input current for no loss system is:

$$I_{dc} = \frac{NI_0}{1-D} \tag{7}$$

In Eq. (7), the input current Idc is controlled by the duty ratio D using Pulse Width Modulation (PWM). The switching frequency is assumed to be 25 kHz to ensure fast operation. For an N-level boost converter, the voltage gain is derived assuming zero average voltage across the inductor L. The expression for the total inductor voltage in the ON–OFF states is given by

$$V_L = D(V_{dc} - I_L R_L) + (1-D)(V_{dc} - V_C - I_L R_L) = 0 \tag{8}$$

where 'I_L' = inductor current, equivalent to'I_{dc}', 'R_L'= inductor resistance. Another phrase is written when switch "S" is turned off; initial term is valid when it turned ON. From Eq. (5), the input DC voltage is written as follows:

$$V_{dc}(D + 1 - D) + I_L R_L(-D - 1 + D) = (1-D)V_C \tag{9}$$

From Eq. (9), we have:

$$V_{dc} = (1-D)V_c + I_L R_L \tag{10}$$

Therefore, from Eq.s (8) to (10), the input voltage, V_{dc}, can be written as follows:

$$V_{dc} = (1-D)\frac{V_0}{N} + \frac{NV_0}{(1-D)R_0} R_L \tag{11}$$

Therefore, from Eq. (11), it can be stated that

$$\frac{V_{dc}}{V_O} = \frac{1}{\frac{1-D}{N} + \frac{NR_L}{(1-D)R_O}} \tag{12}$$

Eq. (12) reduces to Eq. (5) when N=1 and D=0. From Eq. (12), it is observed that the maximum voltage gain is achieved at D=1 and subsequently decreases to zero. The influence of RL introduces constraints on the boost factor. The relationship between the boost factor and duty ratio is analyzed by varying RL in Eq. (12). The TLBC achieves a significantly higher voltage gain compared to conventional boost converters (Rajapandian, B., & Sundarrajan, 2020). For the analysis, the duty ratio is assumed to be 0.5.

The optimal working TLBC duty ratio ranges from 0.4 to 0.6. Eq. for voltage gain is as follows:

$$V_{01} = \left(\frac{1}{1-D}\right) * V_{dc} \quad \text{For voltage gain of two} \tag{13}$$

$$V_{02} = \left(\frac{2}{1-D}\right) * V_{dc} \quad \text{For voltage gain of quadruple} \tag{14}$$

$$V_{03} = \left(\frac{1+D}{(1-D)^2}\right) * V_{dc} \quad \text{For voltage increase of six times} \tag{15}$$

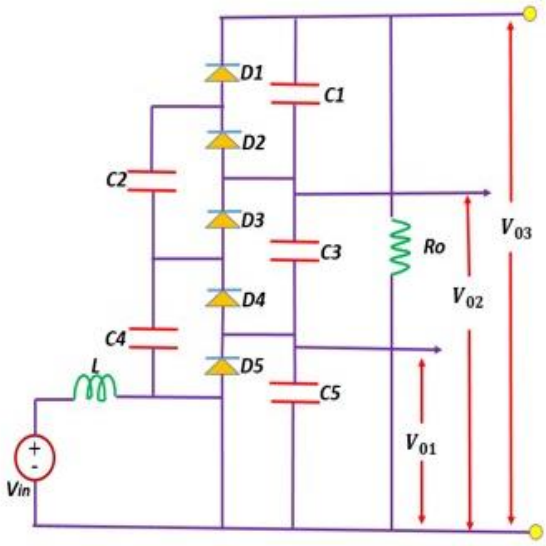

Figure 6. TLBC Configuration.

2.3 Wind powered TLBC with other boost converters

A comparison is made between various boost converters and the TLBC. The different boost converters considered are the traditional boost converter, modified SEPIC, quadratic boost converter, and double-boost converter. Figure 6 shows the variation of voltage gain, or boost factor, with respect to different duty ratios. Compared to the other boost converters, the TLBC achieves the highest voltage gain. From Figure 7, it is observed that at a duty ratio of 0.5, the TLBC attains a significantly higher voltage gain than the other converters.

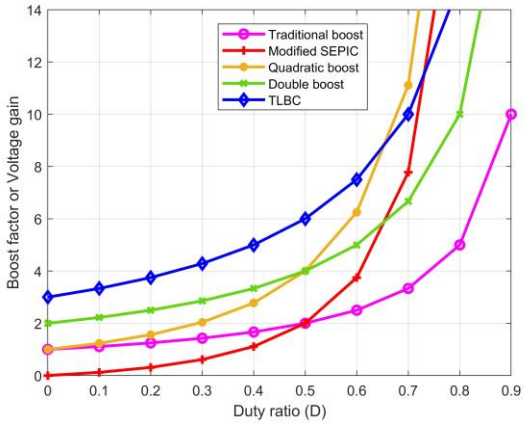

Figure 7. Boost factor of various boost converter with duty ratio.

3. MPPT APPROACHES to WECS

WECS has been receiving significant attention as a renewable energy technology due to its environmental benefits. Wind speed in a WECS fluctuates continuously

throughout the day, and the output power depends on tracking the maximum power at the MPP (Dahmane et al., 2024). Therefore, an appropriate metaheuristic-based MPPT approach is required to extract the maximum output power. The choice of a suitable metaheuristic-based MPPT method is independent of the generator type employed (Bollipo N. et al., 2020). Such an MPPT approach can be implemented at the generator side for effective control. This study focuses on a metaheuristic-based GWO MPPT approach, which is applied to a PMSG-based WECS and compared with the conventional Perturb & Observe (P&O) MPPT method.

3.1 GWO based MPPT Approach

A primary challenge for WECS is its performance under unpredictable weather conditions, which can lead to reduced power generation. Therefore, it is essential to develop an effective metaheuristic-based MPPT approach to extract the desired optimal power. The conventional P&O MPPT method has been applied to PMSG-based WECS and analyzed in (Pranupa S. et al., 2022); however, its performance is often unsatisfactory. The P&O approach can suffer from power losses due to perturbations and fails to track the maximum power point quickly under variable wind speeds. The metaheuristic-based GWO MPPT approach is inspired by the leadership and hunting behavior of grey wolves in nature (Uddin M. N. et al., 2018). This approach is accessible, flexible, and straightforward to implement. It balances exploration and exploitation during the optimization process, resulting in improved system performance. Nevertheless, it also has some limitations, such as unsatisfactory convergence speed and limited population diversity. Unlike the conventional P&O MPPT, which tracks the MPP in a single trial, the GWO-based MPPT continuously tracks the MPP to achieve optimal power. Grey wolves are apex predators that live in packs and organize their hunting through four hierarchical roles: Alpha (α), Beta (β), Delta (δ), and Omega (ω). The α wolf occupies the highest rank, followed by β, δ, and ω wolves. The ω wolves explore diverse regions to enhance global optimization, while the α, β, and δ wolves guide them toward the optimal positions.

Grey wolves encircle the prey during a hunt. This behavior is mathematically represented by the following simulation Eq..

$$\vec{D} = \vec{C} \times \vec{X_p}(t) - \vec{X}(t) \tag{17}$$

$$\vec{X}(t+1) = \vec{X_p}(t) - \vec{A} \times \vec{D} \tag{18}$$

where t = current iterations, D, A, C = co-efficient vectors, X_p= prey positions vector, X= grey wolf vector position, and r_1 and r_2 are stochastic vectors within the interval 0 to 1. Random vectors values are assumed to be 1 and 0.

GWO algorithm fitness function is as follows:

$$P\left(d_i^k\right) > p(d_i^{k-1}) \tag{19}$$

The meta-heuristic-based GWO algorithm is utilized to minimize the fitness function. Procedures for fitness assessment; Create a grey wolf population with N Particles Xi at random from 1, 2, 3,..., n.

Find the fitness value of every grey wolf in population; mark alpha wolf as having the lowest fitness value, beta wolf as having second lowest fitness value, and the delta wolf as having the third lowest fitness value.

Iterate within the range: execute the loop a maximum of max_iter times, determining the value of a = 2 at each step.

The GWO algorithm involves three main behaviors: hunting, attacking prey, and searching for the target. Grey wolves possess the ability to detect prey, with the alpha wolf directing the hunt. The hunting patterns of grey wolves are defined by the following rules:

$$\vec{D_\alpha} = \left|\vec{C_1} \times \vec{X_\alpha} - \vec{X}\right| \tag{20}$$

$$\vec{X_1} = \left|\vec{X_\alpha} - \vec{A_1} \times (\vec{D_\alpha})\right| \tag{21}$$

$$\vec{D_\beta} = \left|\vec{C_2} \times \vec{X_\beta} - \vec{X}\right| \tag{22}$$

$$\vec{X_2} = \left|\vec{X_\beta} - \vec{A_2} \times (\vec{D_\beta})\right| \tag{23}$$

$$\vec{D_\delta} = \left|\vec{C_3} \times \vec{X_\delta} - \vec{X}\right| \tag{24}$$

$$\vec{X_3} = \left|\vec{X_\delta} - \vec{A_3} \times (\vec{D_\delta})\right| \tag{25}$$

The final phase of grey wolf hunting involves attacking the prey, during which the fluctuation range decreases to a. The GWO algorithm updates the positions of all search agents to converge toward the prey. During the exploration phase, grey wolves initially diverge and subsequently converge toward the target (Hajer Gaied et al., 2022).

Figure 8 illustrates the flowchart of the GWO MPPT approach. The GWO is a population-based algorithm that emulates the hierarchical guidance and hunting strategies of grey wolves in the wild.

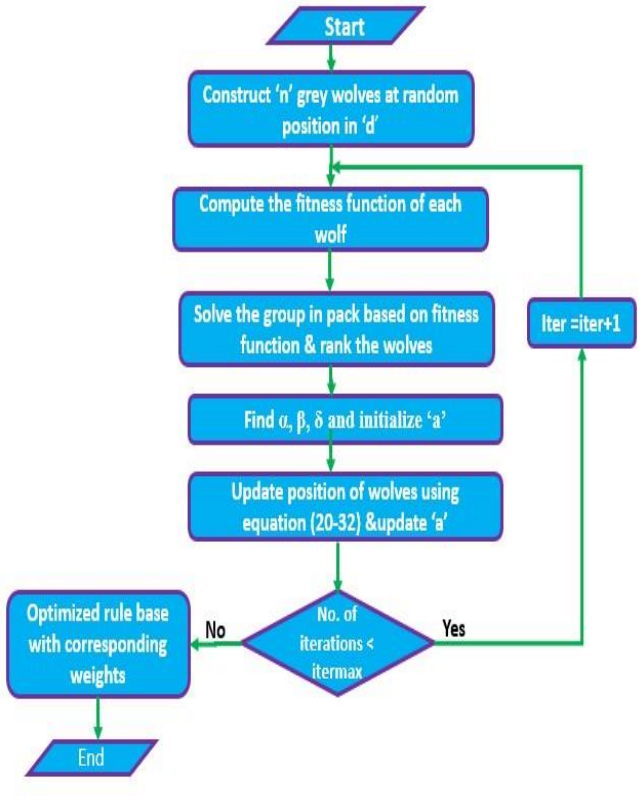

Figure 8. Flow chart of the meta-heuristic based GWO MPPT approach.

The GWO algorithm was proposed by Seyedali Mirjalili (Mirjalili. S. et. al., 2014). Grey wolves, considered apex predators, occupy the highest level of the food chain and typically live in social structures known as packs. Each pack consists of 5 to 12 wolves (Wong L. I. et al., 2014).

Figure 9 illustrates the hierarchical dominance structure of the grey wolf optimizer. The alpha (α) wolf is the leading individual within the pack, and its authority is followed by all

other members. Beta (β) wolves are subordinate wolves that assist the alpha wolf (Yang et al., 2017), representing the most influential members after the alpha. Delta (δ) wolves support the alpha and beta wolves and help manage the omega wolves; they perform roles such as scouts and custodians (Yang et al., 2017). The omega (ω) wolves are the lowest-ranking members of the pack, often serving as scapegoats and given the least priority during feeding. Figure 9 also illustrates the position update process of the grey wolf optimizer. Eq.s (20), (22), and (24) are used to update the positions of the omega wolf and the location vectors of α, β, and δ wolves, respectively.

Here, X denotes the location vector of the current individual. Eq.s (20), (22), and (24) calculate the distances between the current positions of individuals and their respective alpha, beta, and delta positions. The final positions of the vectors are determined by Eq.s (21), (23), and (25).

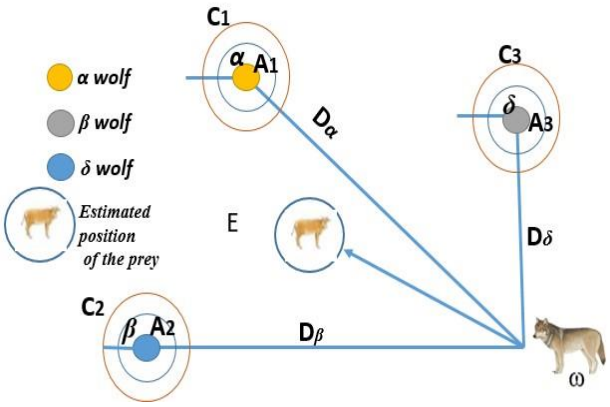

Figure 9. Position updating of grey wolf optimizer.

4. SIMULATION RESULTS OF WIND POWERED TLBC BASED WECS

In this section, the simulation results of the PMSG-based WECS with TLBC using the GWO-based MPPT approach are presented, considering both fixed and variable wind speed profiles. Table 1 provides the parameter specifications of the proposed PMSG and TLBC.

4.1 PMSG fed Rectifier Output under Constant Wind Profile

The DC link voltage of the PMSG-fed uncontrolled rectifier and the corresponding output power are shown in Figure 10 and 11, respectively.

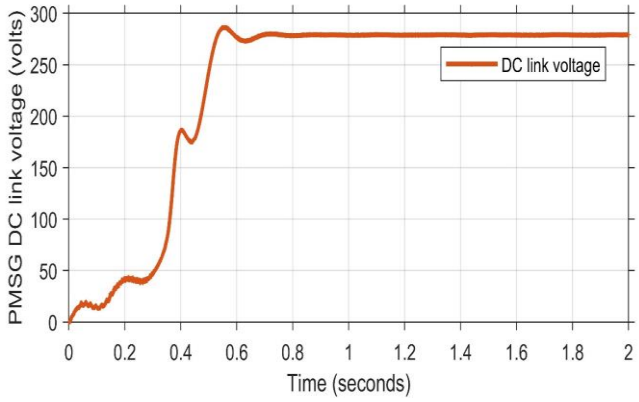

Figure 10. PMSG DC-link voltage at wind profile 10 m/s.

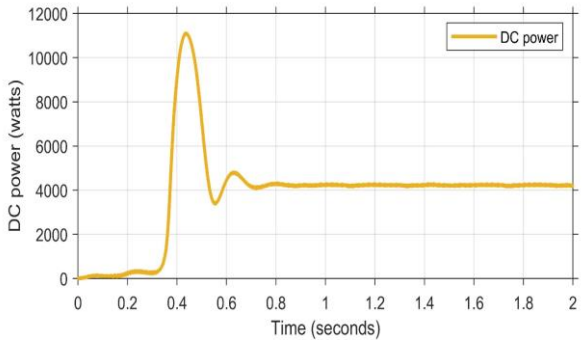

Figure 11. PMSG power output at wind profile 10 m/s.

Table 1. Specifications of PMSG and TLBC.

Si. No	Configuration	Parameters	Values
1	PMSG	Type of the rotor used	3Φ round rotor type
		pole sets	15 poles set
		Speed	300-rpm
		Wind speed	Variation from 2 to 12 m/s
		Air density (ρ)	ρ = 1.225 kg/m
		radius (r)	40 m
2	TLBC	TLBC's C and L	L=1.33 mH, C=100 μF
		Duty ratio (D)	0.5
		Switching frequency	25 kHz
3	GWO	Initial population of wolves	40
		Number of iterations	10
		Number of tasks	500
		Previous solutions	Previous position of wolves
		Xα, Xβ, and Xδ	Current positions of α-wolf, β-wolf, and δ-wolf
		Best solutions	Every wolf with highest fitness
		The creation process of a new solution	Position of α, β and δ
		r1 and r2	Random vectors values between 1 and 0
		Dα, Dβ and Dδ	Distance difference between wolves
		X1, X2 and X3	Traction directions of 3 primary wolves

Figure 12 shows the output voltages of the wind-powered TLBC using the metaheuristic GWO MPPT approach at a wind speed of 10 m/s. The proposed wind-powered TLBC output waveforms, coupled with the PMSG-fed rectifier-based WECS, are analyzed. Figure 13 illustrates the TLBC output power using the GWO MPPT approach at a fixed wind speed of 10 m/s, with the corresponding power output reaching 5200 W. Figure 14 presents the wind-powered TLBC output voltage across the individual DC capacitors C1, C2, and C3 for a duty ratio of 0.5, with respective voltage values of 1666 V, 1110 V, and 552 V.

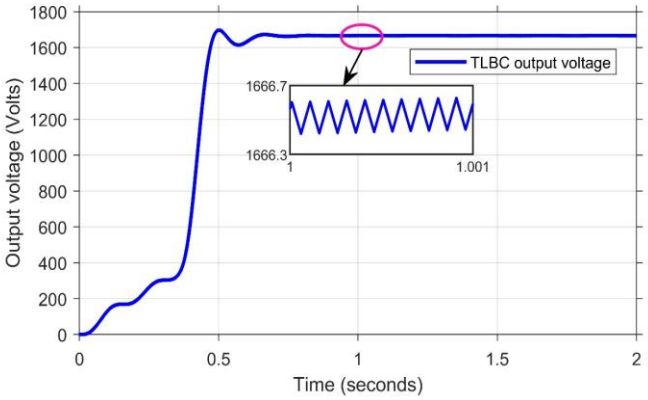

Figure 12. Wind powered TLBC output voltages using GWO at 10 m/s.

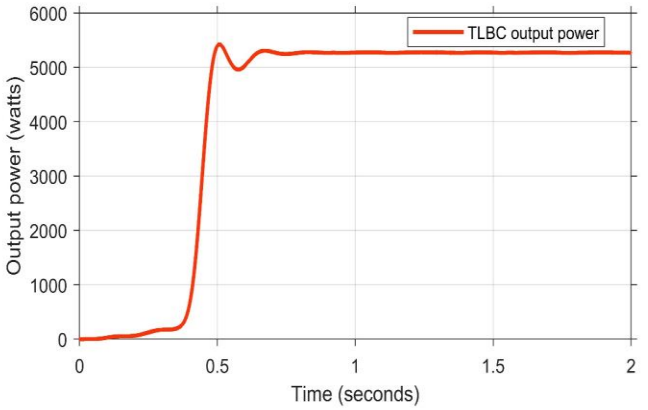

Figure 13. Wind powered TLBC output power using GWO at 10 m/s.

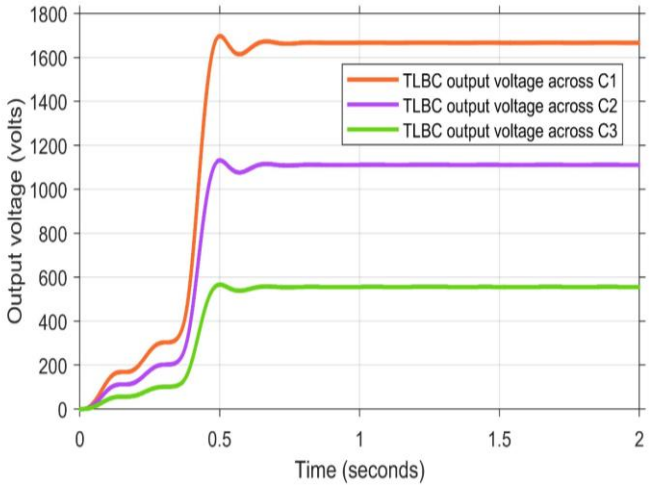

Figure 14. Wind powered TLBC output voltages using GWO at 10 m/s.

4.2 PMSG fed Rectifier output under variable Wind Profile

Figure 15 shows the wind speed profile applied to the PMSG-fed rectifier. A wind speed of 10 m/s is considered from 0 to 2 seconds, 8 m/s from 2 to 4 seconds, and 12 m/s from 4 to 6 seconds.

Figure 16 shows the PMSG DC-link voltage under a variable wind profile. At a wind speed of 10 m/s, the DC-link voltage of the PMSG is 278 V. Similarly, at 8 m/s, the DC-link voltage is 220 V, and at 12 m/s, it reaches 340 V.

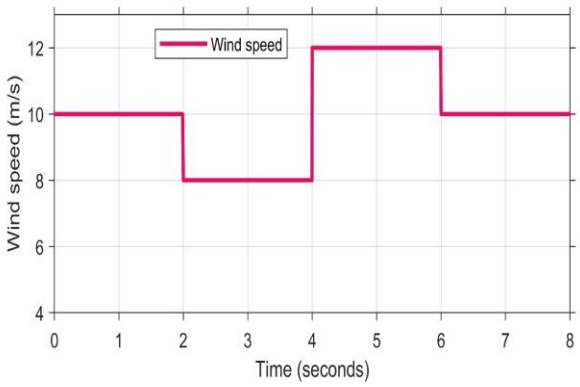

Figure 15. Wind speed profile variation.

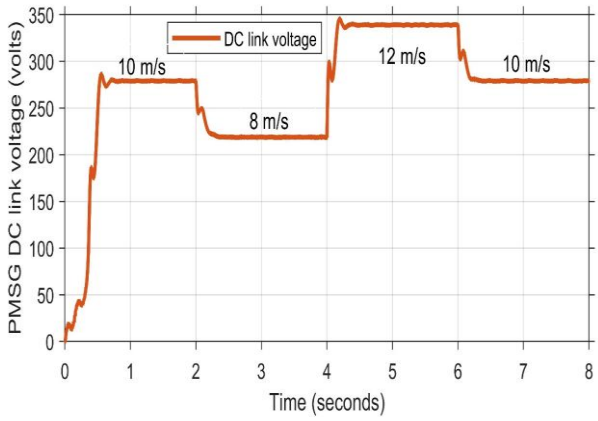

Figure 16. PMSG DC-link voltage under variable wind profile.

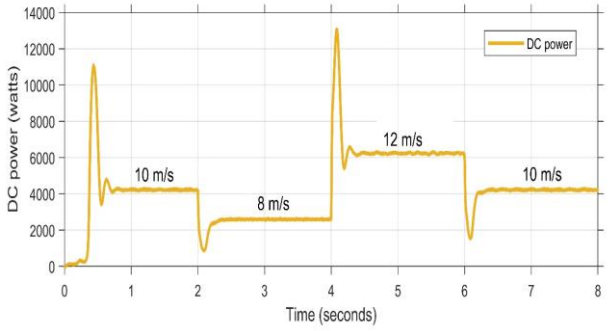

Figure 17. Output power of PMSG under variable wind profile.

Figure 17 shows the output power of the PMSG under variable wind speeds. At a wind speed of 10 m/s, the PMSG output power is 4200 W. At 8 m/s, the output power decreases to 2500 W, while at 12 m/s, it increases to 6800 W. The results of the PMSG-fed rectifier under various wind profiles are summarized in Table 2. These results indicate that the PMSG-fed rectifier produces higher output voltages and power with increasing wind speed. The general parameters for the GWO MPPT approach are provided in Table 2. These vectors are generated randomly (Mirjalili. S. et. al., 2014).

4.3 PMSG Based WECS Interfaced with TLBC

The proposed wind-powered TLBC using the metaheuristic GWO-based MPPT approach is modeled, simulated, and analyzed under both fixed and variable wind speed profiles using MATLAB®/Simulink®. Additionally, its performance is compared with that of the conventional P&O MPPT approach. The performance of the wind-powered

TLBC is evaluated in terms of voltage gain, output ripple, settling time, and the accuracy of the PMSG-based WECS.

Table 2. PMSG fed rectifier under various wind profile results.

Wind Speed (m/sec)	Torque (N-m)	Rotor speed (rad/sec)	PMSG fed rectifier outputs	
			Power (watts)	Voltage (volts)
12	23	290	6800	340
11	21	250	6480	298
10	19.5	240	4200	278
9	17.4	190.8	4064	230
8	14	180	2500	220
7	12.9	141	2215	168.1
6	10.8	110	1520	135.6
4	9	89	930	100.5

4.4 Wind Powered TLBC using GWO MPPT Approach

Furthermore, the performance of the wind-powered TLBC-based WECS with the GWO MPPT approach is analyzed under the variable wind profile shown in Figure 15. Figure 18 presents the TLBC output voltage across each capacitor (C1, C2, and C3using the GWO MPPT approach for wind speeds of 10 m/s, 8 m/s, and 12 m/s, respectively, with a duty ratio of 0.5. In the figure, the orange line represents the TLBC output voltage across C1, the purple line across C2, and the green line across C3.

Figure 19 shows the final TLBC output voltage for the same variable wind speed profile and duty ratio. The corresponding output voltages of the TLBC are 1666 V, 1315 V, and 2038 V for wind speeds of 10 m/s, 8 m/s, and 12 m/s, respectively.

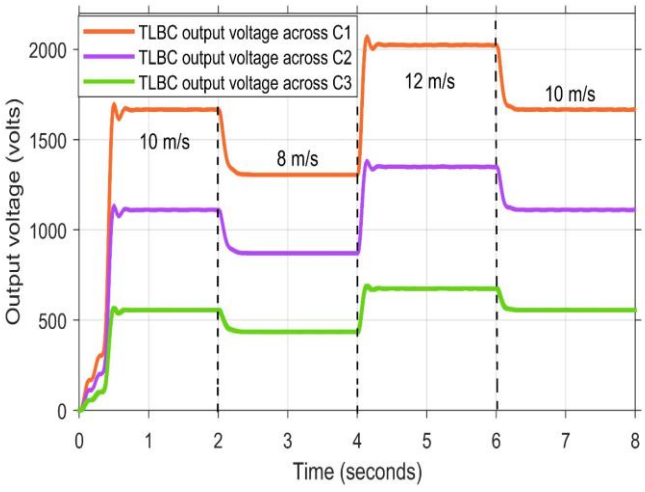

Figure 18. Wind powered TLBC output voltage using GWO under variable wind speeds.

The TLBC output voltages are summarized in Table 3. Figure 20 shows the output power of the wind-powered TLBC using the GWO MPPT approach under a variable wind speed profile of 10 m/s, 8 m/s, and 12 m/s. The corresponding output power values are 5200 W, 3200 W, and 7800 W, respectively.

Furthermore, the performance of the wind-powered TLBC is compared with that of a conventional wind-powered boost converter. From Table 4, it is observed that the proposed wind-powered TLBC achieves an improved voltage gain of 5.98 at a duty ratio of D=5.

The Voltage gain is calculated as $Vgain = \frac{V_{out}}{V_{in}}$ (30)

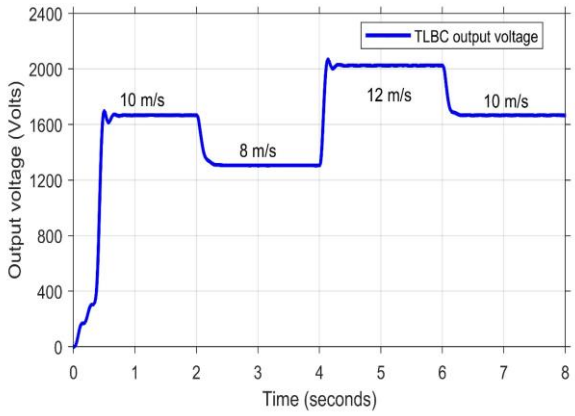

Figure 19. Wind powered TLBC output voltage using GWO under variable wind profile.

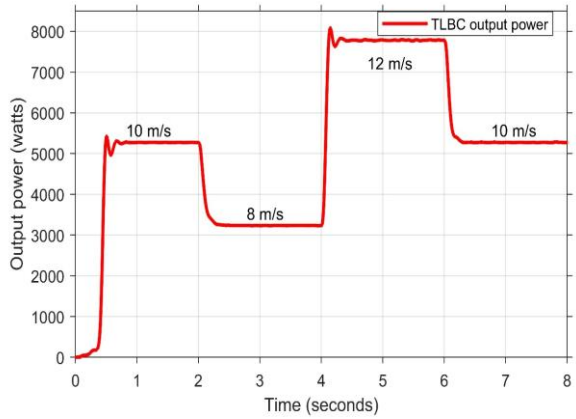

Figure 20. Wind powered TLBC output power using GWO under variable wind profile

Table 3. Wind powered TLBC using GWO MPPT approach.

Wind speed (m/sec)	TLBC outputs			
	Voltage (volts)			Power (watts)
	Input voltage	Conventional Boost Converter	TLBC output voltage	Output power
12	340	678	2038	7800
11	297	574	1723	5883
10	278	554	1666	5200
9	235	459	1371	3754
8	220	435	1315	3200
7	171	343	1027	2090
6	150	286	885	985
4	110	215	652	611

Table 4. Comparison of different MPPT approaches at a fixed wind speed of 10 m/s.

Si. No.	Parameters	GWO	P&O
1	PMSG Voltage (volts)	554	510
2	TLBC Voltages (volts)	1666	1542
3	TLBC Power (watts)	5200	4751
4	Settling time (sec)	0.5	0.2
5	Oscillations	Very Less	More
6	Accuracy (%)	98.99	94
7	Voltage gain	5.996	5.55
9	MPP tracking speed	Less	More

In contrast, the wind-powered conventional boost converter achieves a voltage gain of 1.98, whereas the wind-powered TLBC attains a voltage gain of approximately 6. The wind-powered TLBC using the metaheuristic-based GWO MPPT approach is particularly suitable for HVDC transmission line and EV applications due to its lower ripple content, higher accuracy, and ability to track the optimal power point under variable wind speed profiles. The TLBC provides a voltage gain that is roughly three times higher than that of the conventional boost converter, making it well-suited for PMSG-based WECS employed in HVDC transmission line applications.

5. COMPARISON OF RESULTS

This paper proposes a wind-powered TLBC using a metaheuristic-based GWO MPPT approach for HVDC transmission line applications. The WECS serves as a peak load source for the HVDC line connected to the grid. The system performance is evaluated under both fixed and variable wind speed conditions. The proposed GWO-based MPPT approach demonstrates superior performance compared to the conventional P&O MPPT method.

The performance of the wind-powered TLBC is assessed in terms of voltage gain, output ripple, settling time, output power efficiency, and the accuracy of the PMSG-based WECS. The proposed wind-powered TLBC using the GWO-based MPPT approach achieves a high voltage gain with a boost factor of 5.996, minimal oscillations, improved settling time, and high accuracy of 99% compared to the P&O MPPT method.

The efficiency of the PMSG-based WECS is also improved with the integration of the GWO MPPT and TLBC. Table 4 presents a comparison of the metaheuristic-based GWO MPPT and conventional P&O MPPT approaches, including parameters such as output voltage, settling time, ripple content, accuracy, MPP tracking speed, and voltage gain for the wind-powered TLBC. From Figure 21, it is observed that the P&O MPPT approach exhibits more oscillations, and the TLBC output voltage is 1510 V.

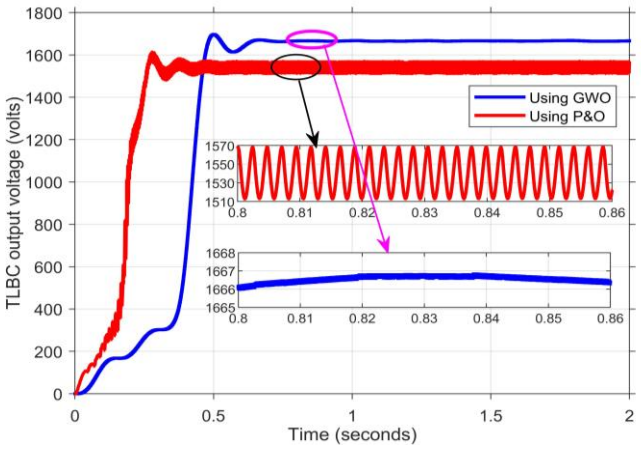

Figure 21. Wind powered TLBC output power using GWO and P&O.

For the wind-powered TLBC using the metaheuristic-based GWO MPPT approach at 10 m/s, the output voltage is 1666 V, with minimal oscillations observed. The settling time for the GWO-based MPPT is 0.5 s, whereas the conventional P&O MPPT exhibits slightly faster settling but with significantly higher oscillations.

The output power obtained with the GWO-based MPPT is higher and more accurate compared to the P&O MPPT. Therefore, the wind-powered TLBC using the metaheuristic-based GWO MPPT approach is highly suitable for HVDC transmission line applications, where a stable, accurate, and low-oscillation voltage is essential for reliable operation.

6. CONCLUSIONS

The proposed PMSG-based WECS coupled with the TLBC utilizing the GWO-based MPPT approach has been analyzed under fixed and variable wind speed profiles of 10, 8, and 12 m/s, with the pitch angle (β\betaβ) set to 0. The results are also compared with the traditional P&O-based MPPT approach. Simulation results indicate that the WECS generates higher voltages as wind speed increases.

For the wind-powered TLBC, the GWO-based MPPT approach achieves an output voltage gain with a boost factor of 5.996 at a wind speed of 10 m/s, whereas the P&O-based MPPT approach achieves a boost factor of 5.55 under the same conditions. In comparison, the traditional wind-powered boost converter achieves a voltage gain of 1.99 with the GWO MPPT and 1.97 with the P&O MPPT at 10 m/s. Thus, the TLBC enhances the output voltage approximately threefold compared to the conventional boost converter.

The GWO-based MPPT approach provides an output power of 5200 W, a settling time of 0.5 s, and an accuracy of 98.99%, with minimal ripple content compared to the P&O method. Consequently, the wind-powered TLBC using the GWO-based MPPT demonstrates superior performance in terms of voltage gain, output stability, and accuracy. Although several other MPPT approaches exist, they are not discussed in this study. In conclusion, for HVDC transmission line applications, the proposed PMSG-based WECS coupled with the TLBC using the GWO-based MPPT approach is highly suitable, offering optimal performance in terms of settling time, voltage stability, and minimal oscillations.

7. ACKNOWLEDGEMENT

The authors thank the Vice Chancellor and Management of MSRUAS, Bangalore for their approval to publish this research.

REFERENCES

1. Ahmad, R., & Abdul-Hussain, M. (2017). Modeling and simulation of wind turbine generator using Matlab-Simulink. *Journal of Al-Rafidain University College For Sciences* (Print ISSN: 1681-6870, Online ISSN: 2790-2293), (2), 282-300. https://doi.org/10.55562/jrucs.v40i2.204

2. Bollipo, R. B., Mikkili, S., & Bonthagorla, P. K. (2020). Critical Review on PV MPPT Techniques: Classical, Intelligent and Optimisation. *IET Renewable Power Generation*, 14(9), 1433–1452. https://doi.org/10.1049/iet-rpg.2019.1163

3. Catalan, P., Wang, Y., Arza, J., & Chen, Z. (2023). A Comprehensive Overview of Power Converter Applied in High-Power Wind Turbine: Key Challenges and Potential Solutions. *IEEE Transactions on Power Electronics*, 1–28. https://doi.org/10.1109/tpel.2023.3234221

4. Dahmane, K., Bouachrine, B., Ajaamoum, M., Imodane, B., Benydir, M., El Idrissi, A., ... & El Aroudi, A. (2024). Fuzzy Logic Based Adaptive P&O MPPT Control of a DC-DC Boost Converter Used in a Wind Energy Conversion System with a Permanent Magnet Synchronous Generator. *IFAC-PapersOnLine*, *58*(13), 587-592. https://doi.org/10.1016/j.ifacol.2024.07.546

5. Das, M., & Agarwal, V. (2016). Design and Analysis of a High-Efficiency DC–DC Converter With Soft Switching Capability for Renewable Energy Applications Requiring High Voltage Gain. *IEEE Transactions on Industrial Electronics*, 63(5), 2936–2944. https://doi.org/10.1109/tie.2016.2515565

6. Hajer Gaied, Mohamed, N., Habib Kraiem, B. Srikanth Goud, Flah Aymen, Alghaythi, M. L., Hossam Kotb, Samia Gharib Ali, & AboRas, K. M. (2022). Comparative analysis of MPPT techniques for enhancing a wind energy conversion system. *Frontiers in Energy Research*, 10. https://doi.org/10.3389/fenrg.2022.975134

7. Haque, M. E., Negnevitsky, M., & Muttaqi, K. M. (2008). A novel control strategy for a variable speed wind turbine with a permanent magnet synchronous generator. *In 2008 IEEE industry applications society annual meeting* (pp. 1-8). IEEE. https://doi.org/10.1109/08IAS.2008.374

8. Kiran, K. B., Indira, M. S., & Nagaraja, R. (2021). Mathematical modeling and evaluation of performance characteristics of a hybrid solar PV and wind energy system. *Journal of Applied Science and Engineering*, *25*(4), 785-797. https://doi.org/10.6180/jase.202208_25(4).0014

9. Mirjalili, S., Mirjalili, S. M., & Lewis, A. (2014). Grey wolf optimizer. *Advances in engineering software*, *69*, 46-61. https://doi.org/10.1016/j.advengsoft.2013.12.007

10. Mohamed, S.A. and Abd El Sattar, M. (2019). A comparative study of P&O and INC maximum power point tracking techniques for grid-connected PV systems. *SN Applied Sciences*, 1(2). https://doi.org/10.1007/s42452-018-0134-4

11. Mousa, H. H. H., Youssef, A.-R., & Mohamed, E. E. M. (2021). State of the art perturb and observe MPPT algorithms based wind energy conversion systems: A technology review. *International Journal of Electrical Power & Energy Systems*, *126*, 106598. https://doi.org/10.1016/j.ijepes.2020.106598

12. Nagaraja Rao, S., Anisetty, S. K., Manjunatha, B. M., Kiran Kumar, B. M., Praveen Kumar, V., & Pranupa, S. (2022). Interleaved high-gain boost converter powered by solar energy using hybrid-based MPP tracking technique. *Clean Energy*, 6(3), 460–475. https://doi.org/10.1093/ce/zkac026

13. Pande, J., Nasikkar, P., Kotecha, K., & Varadarajan, V. (2021). A Review of Maximum Power Point Tracking Algorithms for Wind Energy Conversion Systems. *Journal of Marine Science and Engineering*, *9*(11), 1187. https://doi.org/10.3390/jmse9111187

14. Pranupa, S., Sriram, A. T., & Nagaraja Rao, S. (2024). Wind farm layout optimization approach using bio-inspired meta-heuristic algorithm to minimize wake effect. *International Journal of Dynamics and Control*, *12*(2), 531-550. https://doi.org/10.1007/s40435-023-01172-y

15. Pranupa, S., Sriram, A. T., & Nagaraja Rao, S. (2023). A review of wind farm layout optimization techniques for optimal placement of wind turbines. *Int J Renew Energy Res*, *13*, 957-65. https://doi.org/10.20508/ijrer.v13i2.13935.g8768

16. Pranupa S, Sriram, A. T., & Nagaraja Rao, S. (2022). Wind energy conversion system using perturb & observe-based maximum power point approach interfaced with T-type three-level inverter connected to grid. *Clean Energy*, 6(4), 534–549. https://doi.org/10.1093/ce/zkac034

17. Priyadarshi, N., Ramachandaramurthy, V., Padmanaban, S., & Azam, F. (2019). An Ant Colony Optimized MPPT for Standalone Hybrid PV-Wind Power System with Single Cuk Converter. *Energies*, *12*(1), 167. https://doi.org/10.3390/en12010167

18. Rajapandian, B., & Sundarrajan, G. T. (2020). Evaluation of DC-DC converter using renewable energy sources. *International Journal of Power Electronics and Drive Systems*, 11(4), 1918. https://doi.org/10.11591/ijpeds.v11.i4.pp1918-1925

19. Sarang, S. A., Raza, M. A., Panhwar, M., Khan, M., Abbas, G., Touti, E., & Wijaya, A. A. (2024). Maximizing solar power generation through conventional and digital MPPT techniques: a comparative analysis. *Scientific Reports*, *14*(1), 8944. https://doi.org/10.1038/s41598-024-59776-z

20. Rao, S. N., Ashok Kumar, D. V., & Babu, C. S. (2018). Grid Connected Distributed Generation System with High Voltage Gain Cascaded DC-DC Converter Fed Asymmetric Multilevel Inverter Topology. *International Journal of Electrical & Computer Engineering (2088-8708)*, *8*(6). http://doi.org/10.11591/ijece.v8i6.pp4047-4059

21. Sulake, N. R., Devarasetty Venkata, A. K., & Choppavarapu, S. B. (2018). FPGA implementation of a three-level boost converter-fed seven-level dc-link cascade H-bridge inverter for photovoltaic applications. *Electronics*, *7*(11), 282. https://doi.org/10.3390/electronics7110282

22. Teklehaimanot, Y. K., Akingbade, F. K., Ubochi, B. C., & Ale, T. O. (2024). A review and comparative analysis of maximum power point tracking control algorithms for wind energy conversion systems. *International Journal of Dynamics and Control*, *12*(9), 3494-3516. https://doi.org/10.1007/s40435-024-01434-3

23. Uddin, M. N., Amin, I. K., Rezaei, N., & Marsadek, M. (2018, September). Grey wolf optimization-based power management strategy for battery storage of DFIG-WECS in standalone operating mode. In *2018 IEEE industry applications society annual meeting (IAS)* (pp. 1-7). IEEE. https://doi.org/10.1109/IAS.2018.8544633

24. Veerabhadra, J., & Rao, S. N. (2023). Assessment of hybrid MPPT for SPV based high gain cubic boost converter interfaced with reduced switch multilevel inverter for power quality enhancement. *Engineering Research Express*, *5*(4), 045076. https://doi.org/10.1088/2631-8695/ad0fc1

25. Wong, L. I., Sulaiman, M. H., Mohamed, M. R., & Hong, M. S. (2014). Grey Wolf Optimizer for solving economic dispatch problems. In *2014 IEEE international conference on power and energy (PECon)* (pp. 150-154). IEEE. https://doi.org/10.1109/PECON.2014.7062431

26. Yang, B., Zhang, X., Yu, T., Shu, H., & Fang, Z. (2017). Grouped grey wolf optimizer for maximum power point tracking of doubly-fed induction generator based wind turbine. *Energy conversion and management*, 133, 427-443. https://doi.org/10.1016/j.enconman.2016.10.062